



**Structure of a Site-2 Protease Family Intramembrane Metalloprotease**

Liang Feng, *et al.*  
*Science* **318**, 1608 (2007);  
DOI: 10.1126/science.1150755

***The following resources related to this article are available online at [www.sciencemag.org](http://www.sciencemag.org) (this information is current as of December 10, 2007):***

**Updated information and services**, including high-resolution figures, can be found in the online version of this article at:

<http://www.sciencemag.org/cgi/content/full/318/5856/1608>

**Supporting Online Material** can be found at:

<http://www.sciencemag.org/cgi/content/full/318/5856/1608/DC1>

This article **cites 31 articles**, 11 of which can be accessed for free:

<http://www.sciencemag.org/cgi/content/full/318/5856/1608#otherarticles>

This article appears in the following **subject collections**:

Biochemistry

<http://www.sciencemag.org/cgi/collection/biochem>

Information about obtaining **reprints** of this article or about obtaining **permission to reproduce this article** in whole or in part can be found at:

<http://www.sciencemag.org/about/permissions.dtl>

# Structure of a Site-2 Protease Family Intramembrane Metalloprotease

Liang Feng,<sup>1\*</sup> Hanchi Yan,<sup>1\*</sup> Zhuoru Wu,<sup>1\*</sup> Nieng Yan,<sup>1</sup> Zhe Wang,<sup>2</sup>  
Philip D. Jeffrey,<sup>1</sup> Yigong Shi<sup>1†</sup>

## AUTHORS' SUMMARY

An unusual signaling mechanism involves the cleavage of a transmembrane protein within the lipid membrane bilayer. Cleavage is accomplished by a membrane-embedded protease enzyme (1), so this process is called regulated intramembrane proteolysis (RIP) and is used by organisms from bacteria to humans. The first RIP system to be molecularly characterized was the cleavage of the membrane-anchored transcription factor SREBP (sterol regulatory element-binding protein) by a metalloprotease known as site-2 protease (S2P) (2). This cleavage releases a transcription factor, which translocates into the nucleus of the cell and activates genes involved in synthesis and uptake of cholesterol and fatty acids. How S2P cleaves a protein embedded within the lipid bilayer has been enigmatic. Cleavage of a protein requires water molecules. How does water gain access to the buried active site of S2P? Is the metal ion cofactor that is required for catalysis exposed to the lipid environment? If not, how can a substrate protein get into the active site? Finally, what does an S2P protease look like, and how does the structure support its function? Our study of the S2P protein provides clues for the answers to all these questions.

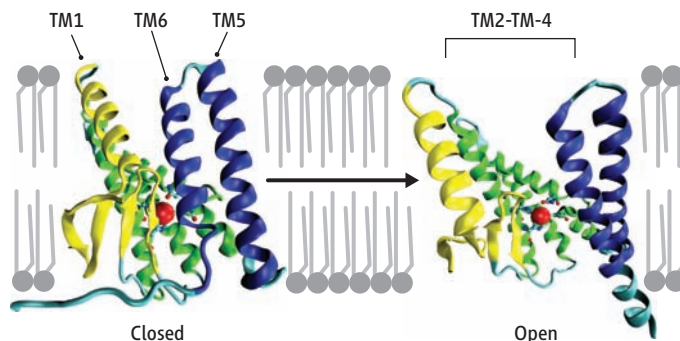
X-ray crystallography is a powerful approach for elucidation of the detailed three-dimensional structure of macromolecules. A prerequisite is generation of crystals that are sufficiently ordered and large enough to produce useful x-ray diffraction data—a daunting challenge for membrane proteins. We were able to crystallize the S2P protein from the archaeobacterial species *Methanocaldococcus jannaschii* by including the detergent decyl- $\beta$ -D-maltopyranoside. To improve the ability of these crystals to diffract x-rays, we incorporated two additional detergents into the crystallization buffer. The structure was determined with multi-wavelength anomalous dispersion.

S2P has six transmembrane segments, TM1 through TM6 (see the figure). The catalytic zinc atom is located ~14 Å from the lipid membrane surface. Zinc is coordinated by three amino acids, His<sup>54</sup> and His<sup>58</sup> in TM2, and Asp<sup>148</sup> in TM3, which are highly conserved in all S2P proteins. TM2 and TM4 are stabilized by TM3, and together, these three segments constitute a core domain of S2P (green). Amino acid sequences for TM2–4 are similar in S2P proteins from other species, which suggests that they have a similar structure and a conserved active-site conformation. In the crystals, two molecules of S2P are contained in one asymmetric unit, the minimal element that can be built into an entire crystal. The two molecules exist in different conformations (see the figure). Although the conformations of the core domain are identical, the other TM segments are quite different; TM1 and TM6 are 10 to 12 Å farther apart in one S2P molecule than in the other. The conformational difference has a direct consequence: The active site is accessible only in the S2P molecule in which TM1 and TM6 are farther apart. Hence, these two conformations likely represent the open and closed states of S2P. In the open state, the cleft between TM1 and TM6 can accommodate a peptide in an extended conformation. Thus, we propose that, to be properly positioned for cleavage, the peptide gains access to the active site of S2P through the lateral movement of TM1 and TM6. In the closed state, water molecules can get to the zinc in the

active site through a hydrophilic channel that opens to the cytoplasmic side of the lipid membrane.

Although our structure suggests how the substrate peptide may get to the active site, further insight must await biochemical experiments. Given the flexibility of TM1, TM5, and TM6, can substrate enter the active site between TM1 and TM2 or between TM6 and the core domain? Although these possibilities cannot be ruled out, they are not supported by available sequence or structural information. Nonetheless, crystals of S2P were generated in the presence of detergents, rather than membrane lipid. Consequently, the influence of detergents on the structure remains to be characterized.

Despite these caveats, the structure of S2P serves as a framework for understanding the function of intramembrane metalloproteases. The sequence conservation among S2P family members suggests that the active site is in a similar position throughout the family. In contrast, substrate proteins are cleaved at different positions along their putative



Closed and open conformations of an S2P metalloprotease, which cleaves its protein substrates within the cell membrane. Substrate peptide is proposed to gain access to the catalytic zinc atom (red sphere) only in the open conformation.

transmembrane helices. This suggests that, before cleavage, S2P must recognize a specific sequence in the substrate to appropriately position the cleavage site. Such recognition does not necessarily occur within the lipid bilayer, as is the case for human S2P and its homolog in *Bacillus subtilis*.

In addition to the S2P family, there are three additional families of intramembrane proteases: serine protease rhomboid, aspartate protease presenilin, and signal peptide peptidase. The mechanisms of water entry and substrate access appear to be similar between S2P and rhomboid, the only other intramembrane protease for which structural information is available. It remains to be seen whether such mechanisms also apply to the aspartate proteases.

### Summary References

1. M. S. Wolfe, R. Kopan, *Science* **305**, 1119 (2004).
2. M. S. Brown, J. Ye, R. B. Rawson, J. L. Goldstein, *Cell* **100**, 391 (2000).

## FULL-LENGTH ARTICLE

**Regulated intramembrane proteolysis by members of the site-2 protease (S2P) family is an important signaling mechanism conserved from bacteria to humans. Here we report the crystal structure of the transmembrane core domain of an S2P metalloprotease from *Methanocaldococcus jannaschii*. The protease consists of six transmembrane segments, with the catalytic zinc atom coordinated by two histidine residues and one aspartate residue ~14 angstroms into the lipid membrane surface. The protease exhibits two distinct conformations in the crystals. In the closed conformation, the active site is surrounded by transmembrane helices and is impermeable to substrate peptide; water molecules gain access to zinc through a polar, central channel that opens to the cytosolic side. In the open conformation, transmembrane helices  $\alpha 1$  and  $\alpha 6$  separate from each other by 10 to 12 angstroms, exposing the active site to substrate entry. The structure reveals how zinc embedded in an integral membrane protein can catalyze peptide cleavage.**

**R**egulated intramembrane proteolysis (RIP) is a conserved signaling mechanism from bacteria to humans (1–8). An essential step of RIP is the site-specific cleavage of a transmembrane signaling protein by a specific membrane-embedded protease within the lipid bilayer. These intramembrane proteases are classified into four families: the metalloprotease site-2 protease (S2P), serine protease rhomboid, and aspartyl proteases presenilin and signal-peptide peptidase (2–4).

RIP signaling is exemplified by cleavage of the membrane-bound transcriptional factor sterol regulatory element-binding protein (SREBP) by S2P in mammals (9–11). In response to low levels of cellular cholesterol, SREBP is translocated from the endoplasmic reticulum (ER) to the Golgi, where it is cleaved at a site that is three amino acids into the transmembrane segment on the cytosolic side (12). This cleavage follows a prior cleavage in the lumen of the Golgi by the site-1 protease (S1P) (13). Consequently, the DNA binding and transactivation domain of SREBP is released from the Golgi membrane and translocated into the nucleus, where it activates transcription of genes that control biosynthesis and uptake of cholesterol and fatty acids. The mammalian S2P is also responsible for cleavage activation of the transcription factor ATF6 (14), which plays a central role in the ER stress signaling. In response to periplasmic stress, the *Escherichia coli* S2P homolog YaeL (also known as RseP) cleaves a transmembrane protein RseA, following an initial cleavage event mediated by the periplasmic serine protease DegS (15). The *Bacillus subtilis* S2P homolog sporulation protein SpoIVFB removes the prosequence from Pro- $\sigma^K$ , which allows the resulting transcription factor to activate genes that are required for sporulation (16, 17).

The S2P family proteases contain a consensus HExxH sequence, in which the two histi-

dine residues are thought to coordinate a zinc atom together with a conserved aspartate residue (1, 18–20). During catalysis, the conserved glutamate residue is thought to activate a zinc-bound water molecule to initiate nucleophilic attack on the scissile peptide bond. These putative catalytic residues are predicted to be located below the lipid membrane surface. In this case, because proteolysis requires water molecules, how do hydrophilic water molecules enter the active site of S2P? More important, how do transmembrane substrate proteins gain access to the active site? Are there common principles that govern different families of intramembrane proteases? These important questions remain unanswered.

Recent structural investigations on the rhomboid serine proteases revealed tantalizing clues about how an intramembrane protease might function (21–24). However, because S2P shares

no apparent sequence homology with rhomboid, information derived from rhomboid proteases cannot be directly applied to the understanding of S2P. In this study, we report the crystal structure of an S2P homolog from the archaeobacterial species *Methanocaldococcus jannaschii*.

**Crystallization of mjS2P.** We cloned 40 S2P homologs from 31 bacterial and archaeobacterial species and examined their expression in *E. coli* (25). On the basis of solution behavior, we focused on the S2P homolog from *M. jannaschii* and generated crystals of its transmembrane core domain (residues 1 to 224), hereafter referred to as mjS2P.

We reconstituted a proteolysis assay in vitro, in which mjS2P cleaved an artificial protein substrate CED-9 (26) in detergent micelles (Fig. 1A, left). Next, quantitative element analysis revealed that zinc is bound to mjS2P in an approximately 1:1 molar ratio. Finally, the metalloprotease-specific inhibitor 1,10-phenanthroline specifically inhibited substrate cleavage in a concentration-dependent manner (Fig. 1A, right). These analyses validated the use of the transmembrane core domain for crystallographic studies.

The structure of mjS2P was determined by multi-wavelength anomalous dispersion (MAD), with the use of seleno-methionine-labeled protein, and refined to 3.3 Å resolution (table S1 and fig. S1). Details of crystallization and structural determination are given in the supporting online materials (25).

**Overall structure of mjS2P.** There are two molecules of mjS2P in an asymmetric unit, designated A and B, which associate with each

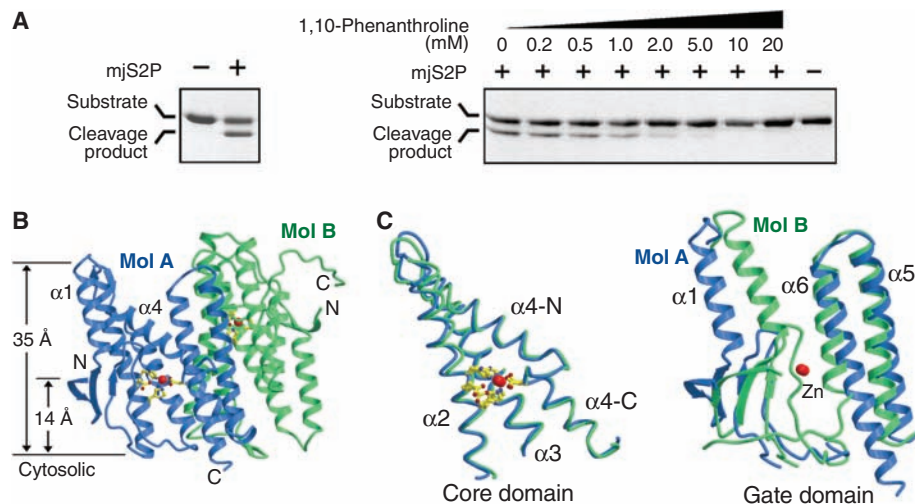


**Fig. 1.** Structure of the transmembrane core domain of an S2P homolog from *M. jannaschii* (mjS2P). (A) The transmembrane core domain of mjS2P is catalytically active. The membrane-associated protein CED-9 (26) was used as an artificial protein substrate for mjS2P. The proteolytic activity is inhibited by 1,10-phenanthroline, an inhibitor specific for metalloproteases (right). (B) Overall structure of mjS2P in one asymmetric unit. Two molecules of mjS2P, named A (blue) and B (green), associate with each other to form a pseudo-dimer in the crystals. The catalytic zinc atom is highlighted in red. The zinc-binding and catalytic residues are colored yellow. (C) The core domain and gate domain of mjS2P. Overlay of the two molecules of mjS2P reveals a shared core domain (left) and a diverging gate domain (right). With the exception of Figs. 3A, 4A, and 4B, all structural figures were made using MOLSCRIPT (30).

<sup>1</sup>Department of Molecular Biology, Lewis Thomas Laboratory, Princeton University, Princeton, NJ 08544, USA.

<sup>2</sup>Department of Chemistry, University of British Columbia, Vancouver, BC V6T 1Z3, Canada.

\*These authors contributed equally to this work.

†To whom correspondence should be addressed. E-mail: ygshi@princeton.edu

other to form an antiparallel, pseudo-dimer in the crystals (Fig. 1B). The orientation of each molecule relative to the lipid membrane was assigned on the basis of the locations of charged amino acids between adjacent transmembrane segments. Each molecule contains seven  $\alpha$  helices and five short  $\beta$  strands (fig. S2). At the N terminus, two antiparallel  $\beta$  strands ( $\beta 1$  and  $\beta 2$ ) combine with a third strand  $\beta 3$ , located between helices  $\alpha 2$  and  $\alpha 3$ , to form a membrane-embedded  $\beta$  sheet. Strands  $\beta 4$  and  $\beta 5$  form a  $\beta$  hairpin between helices  $\alpha 3$  and  $\alpha 4$ -N.

The secondary structural elements of mjS2P are arranged into a six-transmembrane-segment (TM1–6) topology that does not resemble any known metalloprotease (fig. S2). TM1 consists of strand  $\beta 2$  and helix  $\alpha 1$ , whereas TM4 contains two separate  $\alpha$  helices,  $\alpha 4$ -N and  $\alpha 4$ -C, which are connected by a nine-amino acid bulge. TM2, TM3, TM5, and TM6 correspond to helices  $\alpha 2$ ,  $\alpha 3$ ,  $\alpha 5$ , and  $\alpha 6$ , respectively. As previously hypothesized, the catalytic zinc atom is coordinated by three amino acids that are invariant among all S2P family proteins: His<sup>54</sup> and His<sup>58</sup> from helix  $\alpha 2$  and Asp<sup>148</sup> from the N-terminal end of helix  $\alpha 4$ -C in mjS2P. The zinc atom is located  $\sim 14$  Å below the lipid membrane surface from the cytosolic side.

The overall structure of the two mjS2P molecules in one asymmetric unit is similar, with a root-mean-square deviation (RMSD) of 1.8 Å over 150 aligned C $\alpha$  atoms out of a total of 217 amino acids. In particular, TM2, TM3, and TM4 stack closely against each other and share nearly identical conformations in these two molecules (Fig. 1C, left). However, there are also significant conformational differences. Compared with molecule B, molecule A adopts a relatively open conformation, in which TM1 and TM6 move away from each other by approximately 10 to 12 Å (Fig. 1C, right). This difference results in the exposure of the active site in molecule A, but not in B. From these observations, molecules A and B are proposed to exist in open and closed conformations, respectively.

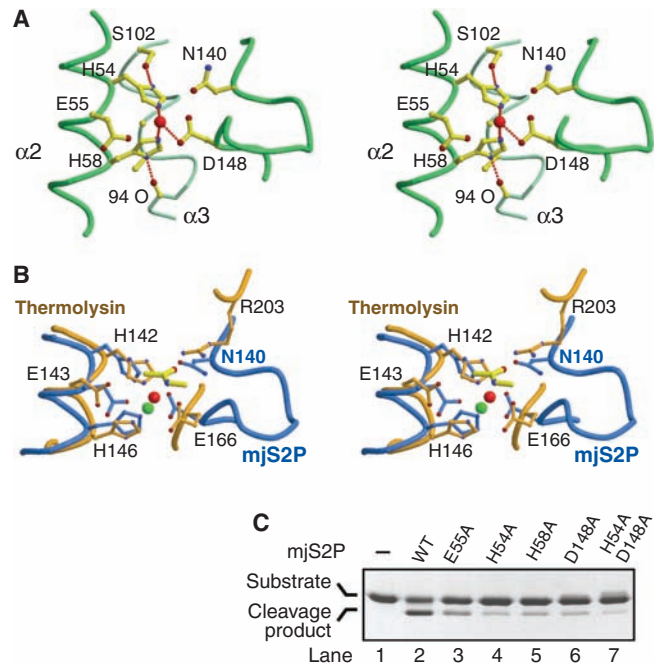
The conserved conformation of TM2 to 4 is likely essential to the formation of the active site, because His<sup>54</sup> and His<sup>58</sup> reside in TM2 and Asp<sup>148</sup> is located in TM4. TM3 plays a structural role by interacting with and supporting the conformations of TM2 and TM4. In support of this analysis, TM2, TM3, and TM4 have been predicted to be common to all S2P family members (19), which contain conserved sequences in these TMs (fig. S2). Thus, we term TM2, TM3, and TM4 the “core domain” of mjS2P. In contrast, TM1, TM5, and TM6 exhibit different conformations in the two mjS2P molecules and may represent two distinct states in the regulation of substrate entry. We thus term TM1, TM5, and TM6 the “gate domain” of mjS2P.

**The active site.** In molecule B, the distances between zinc and the coordinating atoms of His<sup>54</sup>, His<sup>58</sup>, and Asp<sup>148</sup> are 2.3, 2.2, and 2.1 Å,

respectively (Fig. 2A). In molecule A, these distances become 2.3, 2.3, and 2.2 Å, respectively. Coordination of the zinc atom is roughly tetrahedral, with the fourth water ligand unassigned owing to the moderate resolution. In both molecules, His<sup>58</sup> is hydrogen-bonded to the carbonyl oxygen atom of residue 94. The closest carboxylate oxygen atom of Glu<sup>55</sup> is 3.3 and 3.4 Å away from the zinc atom in molecules A and B, respectively. These distances are consistent with activation by Glu<sup>55</sup> of the zinc-bound water molecule during catalysis. It is noteworthy that Asn<sup>140</sup>, another invariant res-

idue among S2P family proteases, is located above the active site in the open space. This location suggests a critical role for Asn<sup>140</sup> in catalysis, perhaps in binding to substrate and/or helping the formation of the oxyanion hole. In support of this notion, comparison of the active-site conformation between mjS2P and thermolysin, a HEXXH-containing metalloprotease, revealed that Asn<sup>140</sup> is located in approximately the same position as Arg<sup>203</sup> in thermolysin (27) (Fig. 2B), which binds to the carbonyl oxygen of the scissile peptide bond and neutralizes the negative charge during catalysis (28).

**Fig. 2.** Conformation of the active site. (A) A stereo view of the active-site conformation in molecule B. The catalytic zinc atom is coordinated by His<sup>54</sup> and His<sup>58</sup> on helix  $\alpha 2$  and Asp<sup>148</sup> at the N-terminal end of helix  $\alpha 4$ -C. Glu<sup>55</sup> likely facilitates the activation of a water molecule during catalysis. The conserved Asn<sup>140</sup> may contribute to the formation of the oxyanion hole. Helix  $\alpha 3$  does not directly participate in catalysis but interacts with helices  $\alpha 2$  and  $\alpha 4$  to form the conserved core domain. (B) A stereo comparison of the active-site conformation between mjS2P (blue) and a HEXXH-containing metalloprotease thermolysin [gold, PDB code 2TLX (27)]. Asn<sup>140</sup> of mjS2P is located in a similar position as Arg<sup>203</sup>



in thermolysin, which is part of the oxyanion hole. (C) Mutation of the active-site residues compromised proteolytic activity. Shown here is an SDS-PAGE gel visualized by Coomassie staining. CED-9 was used as an artificial substrate in these assays.

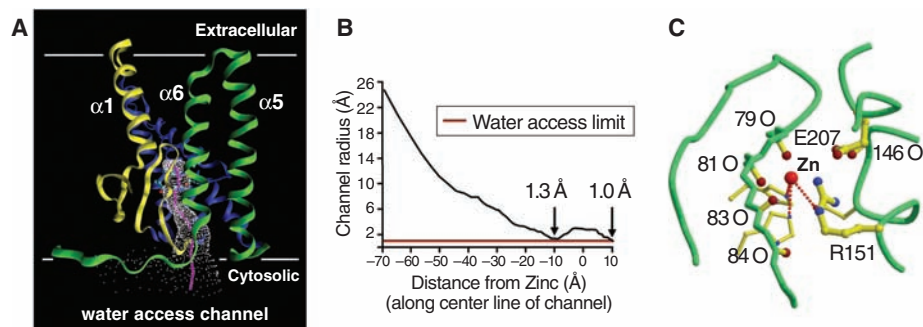


**Fig. 3.** Access of water molecules to the active site of mjS2P. (A) The van der Waals surface in molecule B reveals a channel that leads to the active site from the cytosolic side. The calculation was performed with the program HOLE (31) and the image was generated using VMD (32). The center line of the channel is colored magenta. (B) The channel is large enough to allow passage of water molecules. Distance from the zinc atom along the center line of the channel is plotted against the minimal radius at each point. The red line indicates the minimal radius required for passage of water molecules. (C) The channel is lined with polar groups that may help facilitate water entry. Shown here is a view of the polar groups in the channel approximately along the center line. Five carbonyl oxygen atoms, Arg<sup>151</sup>, and Glu<sup>207</sup> are positioned along the inside of the channel.

To assess the contribution of the catalytic residues, we generated missense mutations in mjs2P. The mutant proteins H54A (in which Ala replaces the His at residue 54), E55A, H58A, D148A, and H54A/D148A (20) exhibited markedly compromised protease activity compared with the wild-type (WT) mjs2P (Fig. 2C). Quantitative element analysis by inductively coupled plasma-emission spectrometry revealed that, compared with the WT protein, the zinc content was 8.2, 44.2, 5.1, and 15.1% for the mutant proteins H54A, E55A, H58A, and D148A, respectively.

An important structural feature of mjs2P is that all active-site residues are contained within TM2 and TM4, with TM3 stabilizing the active-site conformation from the opposite side of where potential substrate proteins are cleaved (Fig. 2A). This arrangement immediately rules out the possibility that conserved residues in TM3 may directly participate in catalysis. Consistent with this analysis, Ala<sup>97</sup> and Gly<sup>98</sup> in the conserved AGxxxN/S/G sequence of TM3 (19) appear to play a structural role in mjs2P. For example, Gly<sup>98</sup> stacks closely against His<sup>54</sup> and His<sup>58</sup>, and its substitution for any other amino acid is predicted to perturb the conformation of the active site because of steric hindrance from the side chain.

**Access to water molecules.** How do water molecules gain access to the active site of mjs2P? Analysis of the van der Waals surface in molecule B reveals a channel that originates from the zinc atom to the cytosolic side (Fig. 3A). The narrowest point in this channel measures  $\sim 2.6$  Å

in diameter (Fig. 3B), which is large enough to allow passage of a water molecule. Notably, the inner surface of the channel contains a number of polar groups and charged amino acids that may facilitate water entry. Five carbonyl oxygen atoms from residues 79, 81, 83, 84, and 146 point into the channel, poised to coordinate water molecules (Fig. 3C). In addition, the side chains of two charged amino acids Arg<sup>151</sup> and Glu<sup>207</sup> also point into the channel. Thus, water molecules appear to have constant access to the active site of mjs2P in the closed conformation.

**Mechanism of substrate entry.** Molecules A and B exhibit markedly different conformations in TM1. In the closed molecule B, exclusively hydrophobic amino acids from TM1 and TM2 interdigitate to form an extensive network of van der Waals interactions (fig. S3A). Compared with molecule B, TM1 (helix  $\alpha 1$  and strand  $\beta 2$ ) pivots outward around helix  $\alpha 2$  by  $\sim 35^\circ$  to reach its position in molecule A (fig. S3B). This movement results in major alteration of the hydrophobic interface between TM1 and TM2. TM6 and TM5 also have different conformations in molecules A and B, although such differences are small compared with those in TM1. Unlike TM1, conformational changes in TM6 and TM5 do not result in the repacking of hydrophobic interfaces, because helix  $\alpha 4$ -C also slightly adjusts its position to maintain the same packing interactions with  $\alpha 6$  and  $\alpha 5$ .

The two contrasting conformations of mjs2P molecules provide a plausible explanation for

the question of how substrate proteins gain access to the active site. In the closed molecule B, the active site is inaccessible to transmembrane protein substrate (Fig. 4A). In the open molecule A, there is a deep groove that is roughly parallel to the transmembrane helices (Fig. 4B). This groove traverses through the entire molecule and exposes the active site to potential substrate peptide. These observations suggest a lateral gating mechanism, in which TM1 and TM6-TM5, as two sides of the gate, move away from each other to allow substrate entry and catalysis (Fig. 4C).

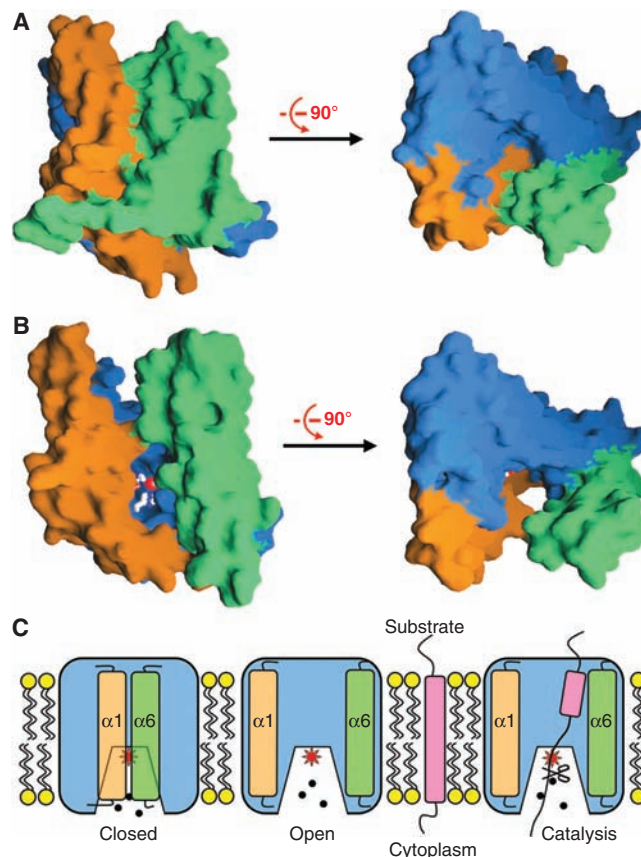
**Discussion.** How is a substrate protein recognized by S2P? Although the current study does not provide a direct answer to this question, it reveals some tantalizing clues. For example, a number of buried amino acids in the closed conformation (molecule B) become exposed in the open conformation (molecule A), thus creating novel surface features that might be involved in binding to substrate proteins. Compared with the bottom half of the putative substrate-binding groove, the top half is much wider (Fig. 4B) and could accommodate an intact  $\alpha$ -helix. We speculate that the funnel-shaped groove in the open conformation may play an active role in unwinding the transmembrane helix of the substrate protein.

Previous studies show that substrate cleavage of the putative transmembrane helix occurs in various positions. These observations appear to contrast with the prediction that the catalytic zinc atom and the active-site residues are likely located in approximately the same depth into the membrane for S2P proteases. This discrepancy can be reconciled by the hypothesis that specific cleavage of a substrate protein is determined by specific recognition.

Structure determination of mjs2P allows comparison with the rhomboid proteases, which represent the only other structurally characterized intramembrane protease (21–24). Despite the superficial similarity of 6TMs, the structures of mjs2P and the rhomboid serine protease GlpG exhibit different topologies and share no apparent features. Nonetheless, water molecules appear to gain access to the active sites of rhomboid and mjs2P via a similar mechanism. GlpG from *E. coli* contains a water-filled cavity that converges on the active-site residue Ser<sup>201</sup> and opens to the extracellular side (21–23). In contrast, mjs2P has a polar channel that allows water entry to the catalytic zinc atom in the closed conformation. Both classes of intramembrane proteases also appear to share a common feature in mechanisms of substrate entry—gating by transmembrane helices, although significant differences exist. In GlpG, bending of the C-terminal half of TM5 was proposed to open the gate for substrate entry (22). This hypothesis is consistent with other structural observations (21, 23, 24) and biochemical characterization (29). In mjs2P, the rotation and translocation of TM1 and the translocation of TM6-TM5 may allow substrate entry.

The full-length mjs2P protein contains 339 amino acids; but only the transmembrane core

**Fig. 4.** Mechanism of substrate gating in mjs2P. (A) Surface representation of the closed state of mjs2P in two perpendicular views. Note the closure of the active site. (B) Surface representation of the open state of mjs2P in two perpendicular views. In this conformation, an extended polypeptide can be readily fitted into the cleft between the two gating helices ( $\alpha 1$  and  $\alpha 6$ ). (A) and (B) were prepared using GRASP (33). (C) A proposed general model for the S2P family of intramembrane proteases. In this model, substrate entry to the active site is gated by two transmembrane segments, TM1 and TM6-TM5.



domain (residues 1 to 224) was used for crystallization. Could the structure be altered or disrupted by not including the C-terminal sequences? Two lines of evidence argue against such a possibility. First, the C-terminal sequences of mjS2P were frequently lost during bacterial expression, which suggests that they are unlikely to be part of the structural core domain. Indeed, the transmembrane core domain of mjS2P was identified by using limited proteolysis. Second, the transmembrane core domain retained full proteolytic activity compared with the full-length mjS2P (fig. S4).

Because mjS2P was crystallized in the presence of detergents, it is possible that the observed conformations are, in part, induced by interactions with the detergent molecules or crystal-packing interactions. Although we could not rule out this possibility, the observed active-site geometry and the conserved core domain structure in the two molecules do not suggest anything had gone awry. Nonetheless, further experiments will determine whether the proposed closed and open conformations of mjS2P in the crystals are physiologically relevant. The large conformational differences of the gate domain in the two molecules are consistent with the fact that TM1 and TM6-TM5 make up highly divergent sequences among members of the S2P family. This feature,

also observed in TM5 of GlpG, would better allow specificity for recognition and cleavage of substrate proteins.

#### References and Notes

1. M. S. Brown, J. Ye, R. B. Rawson, J. L. Goldstein, *Cell* **100**, 391 (2000).
2. S. Urban, M. Freeman, *Curr. Opin. Genet. Dev.* **12**, 512 (2002).
3. M. S. Wolfe, R. Kopan, *Science* **305**, 1119 (2004).
4. J. O. Ebinu, B. A. Yankner, *Neuron* **34**, 499 (2002).
5. M. Ehrmann, T. Clausen, *Annu. Rev. Genet.* **38**, 709 (2004).
6. R. B. Rawson, *Essays Biochem.* **38**, 155 (2002).
7. H. Makinoshima, M. S. Glickman, *Microbes Infect.* **8**, 1882 (2006).
8. S. Urban, *Genes Dev.* **20**, 3054 (2006).
9. J. Sakai *et al.*, *Cell* **85**, 1037 (1996).
10. M. S. Brown, J. L. Goldstein, *Cell* **89**, 331 (1997).
11. R. B. Rawson, *Mol. Cell* **1**, 47 (1997).
12. E. A. Duncan, U. P. Dave, J. Sakai, J. L. Goldstein, M. S. Brown, *J. Biol. Chem.* **273**, 17801 (1998).
13. J. Sakai *et al.*, *Mol. Cell* **2**, 505 (1998).
14. J. Ye *et al.*, *Mol. Cell* **6**, 1355 (2000).
15. B. M. Alba, J. A. Leeds, C. Onufryk, C. Z. Lu, C. A. Gross, *Genes Dev.* **16**, 2156 (2002).
16. D. Z. Rudner, P. Fawcett, R. Losick, *Proc. Natl. Acad. Sci. U.S.A.* **96**, 14765 (1999).
17. Y. T. Yu, L. Kroos, *J. Bacteriol.* **182**, 3305 (2000).
18. A. P. Lewis, P. J. Thomas, *Protein Sci.* **8**, 439 (1999).
19. L. N. Kinch, K. Ginalski, N. V. Grishin, *Protein Sci.* **15**, 84 (2006).
20. Single-letter abbreviations for the amino acid residues are as follows: A, Ala; C, Cys; D, Asp; E, Glu; F, Phe;

G, Gly; H, His; I, Ile; K, Lys; L, Leu; M, Met; N, Asn; P, Pro; Q, Gln; R, Arg; S, Ser; T, Thr; V, Val; W, Trp; X, any amino acid; and Y, Tyr.

21. Y. Wang, Y. Zhang, Y. Ha, *Nature* **444**, 179 (2006).
22. Z. Wu *et al.*, *Nat. Struct. Mol. Biol.* **13**, 1084 (2006).
23. A. Ben-Shem, D. Fass, E. Bibi, *Proc. Natl. Acad. Sci. U.S.A.* **104**, 462 (2007).
24. M. J. Lemieux, S. J. Fischer, M. M. Cherney, K. S. Bateman, M. N. James, *Proc. Natl. Acad. Sci. U.S.A.* **104**, 750 (2007).
25. Materials and methods are available as supporting material on *Science* online.
26. M. O. Hengartner, H. R. Horvitz, *Cell* **76**, 665 (1994).
27. A. C. English, S. H. Done, C. R. Groom, R. E. Hubbard, *Proteins* **37**, 628 (1999).
28. B. M. Matthews, *Acc. Chem. Res.* **21**, 333 (1988).
29. R. P. Baker, K. Young, L. Feng, Y. Shi, S. Urban, *Proc. Natl. Acad. Sci. U.S.A.* **104**, 8257 (2007).
30. P. J. Kraulis, *J. Appl. Cryst.* **24**, 946 (1991).
31. O. S. Smart, J. M. Goodfellow, B. A. Wallace, *Biophys. J.* **65**, 2455 (1993).
32. W. Humphrey, A. Dalke, K. Schulten, *J. Mol. Graph.* **14**, 33 (1996).
33. A. Nicholls, K. A. Sharp, B. Honig, *Proteins Struct. Funct. Genet.* **11**, 281 (1991).
34. We thank A. Saxena at Brookhaven National Laboratory, National Synchrotron Light Source beamlines for help. The atomic coordinates of the transmembrane core domain of mjS2P have been deposited in the Protein Data Bank with the accession code 3B4R.

20 September 2007; accepted 29 October 2007  
10.1126/science.1150755

## REPORTS

# A Cosmic Microwave Background Feature Consistent with a Cosmic Texture

M. Cruz,<sup>1,2\*</sup> N. Turok,<sup>3</sup> P. Vielva,<sup>1</sup> E. Martínez-González,<sup>1</sup> M. Hobson<sup>4</sup>

The Cosmic Microwave Background provides our most ancient image of the universe and our best tool for studying its early evolution. Theories of high-energy physics predict the formation of various types of topological defects in the very early universe, including cosmic texture, which would generate hot and cold spots in the Cosmic Microwave Background. We show through a Bayesian statistical analysis that the most prominent 5°-radius cold spot observed in all-sky images, which is otherwise hard to explain, is compatible with having been caused by a texture. From this model, we constrain the fundamental symmetry-breaking energy scale to be  $\phi_0 \approx 8.7 \times 10^{15}$  gigaelectron volts. If confirmed, this detection of a cosmic defect will probe physics at energies exceeding any conceivable terrestrial experiment.

The Cosmic Microwave Background (CMB) radiation was emitted from the hot plasma of the early universe roughly 14 billion years ago. All-sky, multifrequency maps of the CMB sky made by the Wilkinson Microwave Anisotropy Probe (WMAP) (1, 2) reveal Gaussian temperature anisotropies of the form expected in standard cosmological scenarios, tracing density variations of one part in a hundred thousand in the primordial cosmos (3). However, several apparent anomalies in the expected Gaussian, isotropic statistical distribution have also

been found (4–10). One of the most striking is a large cold spot centered on Galactic coordinates  $b = -57^\circ$ ,  $l = 209^\circ$ , with a radius of  $\approx 5^\circ$  (10–13). It was detected using the Spherical Mexican Hat Wavelet (SMHW), an optimal tool for enhancing such features, and has a flat frequency spectrum, inconsistent with either Galactic foregrounds or the Sunyaev-Zel'dovich effect (13). A conservative estimate of the probability of finding such a feature in Gaussian simulations, taking the effect of a posteriori selection into account, is only 1.85%. Several radical explanations, such as huge

voids or an anisotropic cosmology, have already been proposed: Many have been ruled out by other cosmological observations (14–17).

Here, we consider the possibility that the spot was caused by a cosmic texture (18), a type of cosmic defect predicting spots in the CMB (19). Cosmic defects are hypothetical remnants of symmetry-breaking phase transitions in the early universe, predicted by certain unified theories of elementary particle physics. According to these theories, the different species of elementary particle are indistinguishable in the hot early universe. As the universe cools, the symmetry between them breaks, in a phase transition analogous to the freezing of water. Just as misalignments in the crystalline structure of ice lead to defects, misalignments in the symmetry breaking in unified theories lead to the formation of cosmic defects (20, 21). Breaking a discrete symmetry produces domain walls and breaking a circle [or  $U(1)$ ] symmetry produces cosmic strings. Textures form when a

<sup>1</sup>Instituto de Física de Cantabria, Consejo Superior de Investigaciones Científicas Univ. de Cantabria, Avenida los Castros, 39005-Santander, Spain. <sup>2</sup>Departamento de Física Moderna, Universidad de Cantabria, Avenida los Castros, 39005-Santander, Spain. <sup>3</sup>Department of Applied Mathematics and Theoretical Physics, Center for Mathematical Sciences, Wilberforce Road, Cambridge CB3 0WA, UK. <sup>4</sup>Astrophysics Group, Cavendish Laboratory, J. J. Thomson Avenue, Cambridge CB3 0HE, UK.

\*To whom correspondence should be addressed. E-mail: cruz@ifca.unican.es